

Automatic Detection and Quantification of Non-Viable Myocardium in Late Enhancement Images

A. Hennemuth¹, A. Seeger², O. Friman¹, S. Miller², and H-O. Peitgen¹

¹MeVis Research, Bremen, Bremen, Germany, ²Department of Radiology, University Hospital Tübingen, Tübingen, Baden-Württemberg, Germany

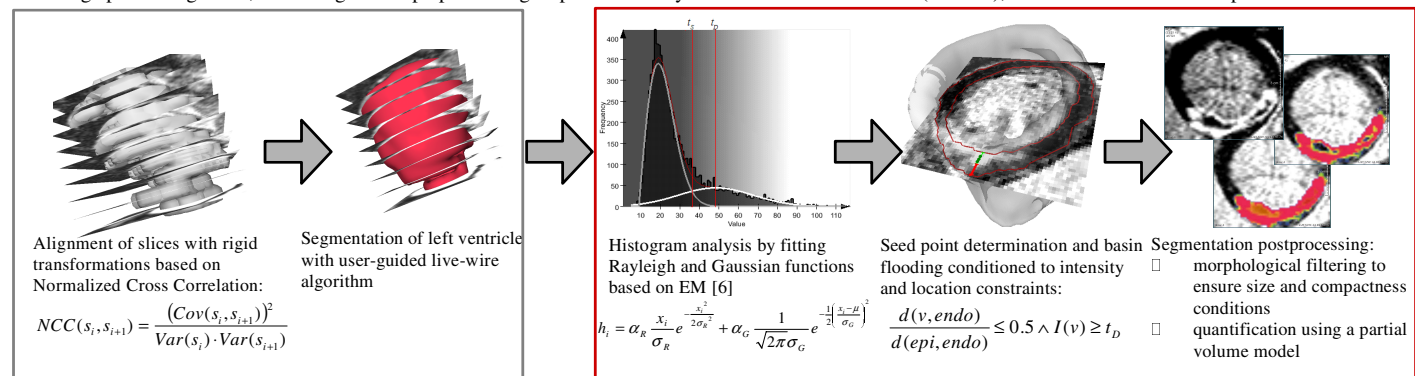
Introduction

Coronary artery disease, especially ischemia of the myocardium is among the main causes of death in western countries. For long-term prognosis, therapy planning and monitoring, the assessment of the infarct size and location is important. Late enhancement (LE) of myocardial tissue after gadolinium contrast agent injection correlates well with fibrosis and can thus be used for the detection and quantification of ischemia [1]. Though there are several approaches for the automatic detection of suitable thresholds for LE detection, only few incorporate further knowledge in the segmentation process [2]. The purpose of our work is the development of a robust automatic method to segment and quantify LE based on some fundamental assumptions about the characteristics of interesting regions:

1. The myocardial surface is smooth
2. The image intensity values inside the myocardium are distributed according to the Rice distribution [3]
3. Late enhancement is most likely to appear in the medial or endocardial part of the myocardium
4. Relevant LE regions are compact crescent-shaped areas of a certain size
5. Dark regions surrounded by LE tissue are no-reflow-areas and thus belong to scarred tissue

Methods

The image processing chain, consisting of two preprocessing steps followed by an automatic LE detection (red box), is derived from the assumptions above:



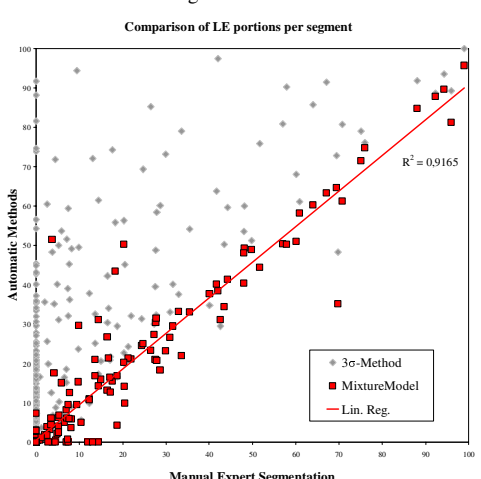
The intensity distribution inside the segmented myocardium is modelled as a mixture of two special cases of the Rice distribution: a Rayleigh distribution representing healthy myocardium and a Gaussian distribution representing the LE tissue [4]. Based on this analysis, intensity thresholds for LE detection t_D and segmentation t_S as well as a partial volume model for volume quantification can be derived. Seed voxels v , that satisfy intensity and location constraints are used to determine the suitable basins of the watershed transform. Resulting clusters are then post-processed to match conditions 4 and 5.

Results

The described methods were applied to 15 short axis datasets of patients with and without ischemia acquired with an inversion recovery turbo flash sequence in clinical routine at 1.5 Tesla (Siemens Avanto) and 3 Tesla (Siemens Trio) and showing varying image quality. Results of the automatic segmentation were controlled by an expert and corrected if necessary. Furthermore, the 3σ -method [5] was applied. The comparison of the determined volumes per segment is shown in the diagram below, the correlation between manual and expert segmentation was 0.96. The overlap between automatic and manual segmentation was measured by the Dice coefficient D which has values between 0.73 and 0.98 in the datasets with segmented clusters from both methods. For overlapping clusters additionally the mean surface distance was derived (see table).

Discussion and Conclusions

The results show a good correlation between the automatic and the expert segmentation, especially compared to the common 3σ -method.



The inspection of the difference voxelsets indicates that deviations mainly occur at the cuspidal ends of crescent-shaped clusters. Outliers occur in regions where data is distorted by artifacts (mainly segments 12-16) and in one dataset, where the expert was not sure, but the consideration of the perfusion analysis approved a distortion in the automatically segmented region. The results show the general applicability of the presented method. The increased uncertainty in the apical segments indicates that long axis images should be included in the analysis. Segmentation accuracy will further be improved by an advanced histogram analysis [4].

References

- [1] Kim RJ et al. NEJM 2000; 343(20):1445-1453.
- [2] Hsu LY et al.. JMRI 2006; 23(3):298-308.
- [3] Gudbjartsson H, Patz S. MRM 1995; 34(6):910-914.
- [4] Friman, O et al. ISMRM 2008, submitted
- [5] Kolipaka, A et al, IJCVI 2005
- [6] Kim DJ, Park DJ. IJSS 2001; 32(8):1075-1087.

Pat	Dice Coeff	ØSurf Dist	Std Dev
1	0.90	1.52	0.16
2	0.95	1.65	0.55
3	0.79	1.55	0.28
5	1.00	-	-
6	0.97	1.74	0.83
7	0.94	2.66	2.40
8	0.00	-	-
9	0.98	1.50	0.00
10	0.97	4.50	4.07
11	0.75	4.26	4.07
12	0.97	2.58	2.85
13	1.00	-	-
14	0.96	1.99	0.77
15	0.73	1.85	1.24
16	0.74	3.25	2.19

Table: Overlap measurement using Dice coefficient D and surface distances with

$$D = \frac{2|V_{exp} \cap V_{auto}|}{|V_{exp}| + |V_{auto}|}$$